Neuron, Vol. 16, 641–651, March, 1996, Copyright ©1996 by Cell Press

Acceleration of Membrane Recycling by Axotomy of Cultured Aplysia Neurons

Uri Ashery,* Reinhold Penner,† and Micha E. Spira*
*Department of Neurobiology
Life Sciences Institute
The Hebrew University of Jerusalem
The Interuniversity Institute for Marine Sciences
of Eilat
Israel
†Max-Planck-Institut fur Biophysikalische Chemie
Gottingen
Germany

Summary

The rapid transition of a stationary axon into a motile growth cone requires the recruitment of membrane and its strategic insertion into the neurolemma. The source of membrane to support the initial rapid growth postaxotomy is not known. Using membrane capacitance measurements, we examined quantitative aspects of membrane dynamics following axotomy of cultured Aplysia neurons. Axotomy activates two processes in parallel: membrane retrieval and exocytosis. Unexpectedly, membrane retrieval is the dominant process in the majority of the experiments. Thus, while a growth cone is vigorously extending, the total neuronal surface area decreases. We suggest that the initial rapid extension phase of the newly formed growth cone postaxotomy is supported by a pool of intracellular membrane that is rapidly retrieved from the neurolemma.

Introduction

The stable structure and surface area of adult neurons can be transiently or permanently altered by external stimuli of various forms. For example, action potentials and chemical stimuli that trigger neurotransmitter or hormonal release by the fusion of intracellular vesicles with the plasma membrane transiently increase the cell surface area (Ceccarelli et al., 1973; Heuser and Reese, 1973; Fernandez et al., 1984; Thomas et al., 1990; Lindau et al., 1992). This increased surface area can spontaneously recover by membrane retrieval processes (Ceccarelli et al., 1973; Heuser and Reese, 1973; Lindau et al., 1992; Heinemann et al., 1994; Thomas et al., 1994).

During development, the neuronal membrane surface area increases while endocytotic activity continuously takes place at the growth cone (GC) level (Wessells et al., 1974; Matteoli et al., 1992). Under these circumstances, the rate of new membrane insertion into the neurolemma must be faster than membrane retrieval. Thus, the neuronal surface area continuously increases (Bray, 1973; Johnston and Wessells 1980, Hochner and Spira, 1987; Pfenninger and Friedman, 1993). Episodes of rapid and localized retraction of GCs, which may be associated with accelerated membrane retrieval, have been observed in response to external stimuli such as the application of specific neurotransmitters (Haydon et al., 1987; Kater and Mills, 1991) or the presentation of specific antigens (Keynes and Cook, 1992; Bandtlow et al., 1993). Thus, the balance between membrane retrieval and insertion may be fine-tuned by external stimuli and thereby modulate the rate of neuronal growth.

Re-growth of adult neurons has been reported to occur in relation to regeneration after injury (Fawcett and Keynes, 1990) and in certain forms of learning and memory (for reviews, see Bailey and Kandel, 1993, 1994).

Axonal injury in the form of axotomy is often followed by resealing of the cut end (Lucas et al., 1985; Fishman et al., 1990; Benbassat and Spira, 1993, 1994; Spira et al., 1993, Ziv and Spira, 1993, 1995; Krause et al., 1994), the formation of a GC (Shaw and Bray, 1977; Bray et al., 1978; Wessells et al., 1978; Baas and Heidemann, 1986; Benbassat and Spira, 1993), and vigorous growth (Bray, 1992). The rapid transition of a differentiated stationary axonal structure into a motile and actively extending GC requires, among other processes, the recruitment of membrane and its strategic insertion into the neurolemma. The sources of membrane to support the rapid initial growth postaxotomy are not known. The transition time between axotomy and GC extension is in some cases so rapid (5–30 min; Bray et al., 1978; Wessells et al., 1978; and the present report) that it is unlikely to involve the activation of membrane synthesis and shipping of vesicles from the cell body. It is more probable that it utilizes preexisting substrates. This is supported by the observations that anucleated distal axonal segments may also extend GCs and neurites postaxotomy (Shaw and Bray, 1977; Baas and Heidemann, 1986; Benbassat and Spira, 1993, 1994). These observations suggest that GC formation and neurite extension may be supported for a limited time by membrane stores within the axons, or alternatively by retrieval of membrane at some locations and its subsequent insertion at others. Another possible source could be the unfolding of membrane invaginations.

Earlier studies aimed at understanding the membrane dynamics associated with GC formation and neurite extension used morphological and biochemical methods (Bray, 1970; Bunge, 1977; Feldman et al., 1981; Griffin et al., 1981; Cheng and Reese, 1987; Pfenninger and Friedman, 1993; Popov et al., 1993). These studies did not provide any quantitative information as to the balance between the endo- and exocytotic activity associated with growth. In fact, it was generally accepted that during growth cone extension the exocytotic activity must be the dominant process.

In the present study, we applied the whole-cell patch-clamp membrane capacitance measurement technique (Hamill et al., 1981; Lindau and Neher, 1988; Penner and Neher, 1989) to examine quantitative aspects of membrane dynamics following axotomy in cultured Aplysia neurons. In contrast to what was expected, we found that axotomy activates, in parallel, membrane retrieval and exocytosis. In the majority of the experiments, the processes of membrane retrieval quantitatively dominated. Thus, while vigorous extension of GC lamellipodium was visualized, the total membrane surface area as expressed by its capacitance decreased.

The presence of extracellularly applied horseradish peroxidase conjugated to wheat germ agglutinin (WGA-HRP) in intracellular organelles revealed that the retrieved membrane accumulated at the central region of the GC. We suggest that the initial rapid extension of the newly formed GC postaxotomy is supported by a pool of intracellular membrane that is formed by enhanced retrieval of the neuronal membrane and its subsequent insertion into the growth cone membrane.

Results and Discussion

Alterations of Membrane Surface Area of Cultured Neurons during Continuous Patch-Clamp Recordings

As a baseline for the present study, we first examined whether long-term patch-clamp recording from intact cultured neurons is associated with alterations in the neurons' membrane surface area. To that end, neurons were cultured on glass-bottomed dishes that were not coated with poly-L-lysine. Under these conditions, the isolated neurons did not extend long neurites, and thus some of them were isopotential and suitable for membrane capacitance measurements. Continuous recording of the membrane capacitance of these neurons ($n = 11$) revealed a net averaged decrease of 4.4% in membrane capacitance over a period of 30 min (Figure 1A). The decrease in membrane capacitance is monotonic over time and might be due to subtle shifts in the balance of exo- and endocytosis during the perfusion of the cytoplasm by the patch-pipette solution.

Induction of Membrane Retrieval by Axotomy in Nongrowing Transected Neurons

To examine the effects of axonal transection on membrane recycling, we measured the membrane capacitance during axotomy and throughout its recovery period. For these experiments, a neuron was patched a few minutes prior to axotomy; its axon was then transected (Spira et al., 1993; Ziv and Spira, 1993, 1995; Benbassat and Spira, 1994), while continuously monitoring the holding current, membrane capacitance, access resistance, and input resistance. In most of the experiments, prior to axonal transection the cultured neurons were not isopotential. Therefore, the whole-cell patch-clamp measurements could not provide accurate membrane capacitance values. However, axotomy eliminated a significant portion of the distal axon, and thus the remaining proximal part of the neuron became an isopotential structure. Under these conditions, the membrane capacitance measurements were reliable.

The alterations in membrane capacitance during axotomy and the recovery period are illustrated in Figures 1B–1D. Axonal transection was associated with a substantial decrease in the neuronal capacitance (Figure 1B) and a transient increase in the inward holding currents (Figure 1C). The transient increase in the holding current corresponds to the rupturing and resealing of the axonal membrane as was analyzed by current-clamp and calcium imaging experiments in our laboratory (Benbassat and Spira, 1993, 1994; Spira et al., 1993; Ziv and Spira, 1993, 1995). The large decrease in the neuron's membrane capacitance monitored immediately after the resealing of the cut end (from 640 pF to 468 pF; Figure 1B) corresponded to the reduction in the physical dimensions of the neuron.

Monitoring of the membrane capacitance following the formation of a membrane seal over the cut end in neurons that did not extend GCs revealed a continuous reduction in the membrane surface area. For example, in the experiment illustrated in Figure 1B–1D, the capacitance decreased after the formation of a membrane seal from 468 pF to 350 pF (Figure 1B and 1D), i.e., over 20% of the membrane surface area underwent endocytosis within 30 min. In this experiment, as well as in other experiments of the same kind, the decreased capacitance appeared to occur in two steps. An initial phase with a time constant of 57 s (ranging in other experiments between 40 and 600 s; average = 241.7 s; SD = 153; $n = 22$) and a second, slower phase with a time constant of 1325 s (ranging between 1000 and 2800 s; average = 1866 s; SD = 548; $n = 21$). The rates of membrane retrieval (fast and slow) postaxotomy are faster than that monitored in the control experiments (Figure 1A). Thus, it is reasonable to assume that both phases are directly related to axotomy.

After the formation of a membrane seal over the cut end (as indicated by the recovery of the holding current), the neuron described by Figures 1B–1D gradually "lost" ~120 pF of its membrane surface area. Assuming that the specific membrane capacitance is 1 $\mu F/cm^2$, the neuron lost ~12,000 μm^2 at an average rate of 400 μm^2/min. Electron microscopic studies (Figure 2) revealed that the endocytotic activity postaxotomy is associated with the appearance of coated pits and vesicles with a diameter of 70–100 nm. Thus, the retrieval of a single vesicle (of 100 nm in diameter) decreases the surface area by 0.03 μm^2. To account for the observed decrease, 380,000 vesicles should have been pinched-off during 30 min, at an average rate of 210 vesicles per second. This rate of endocytosis is well within the range of endocytotic activity observed in other cells. For example, Marsh and Helenius (1980) reported that BHK cells recycle about 100 μm^2 of the cell's surface area per minute.

We identified the location of membrane retrieval and accumulation by following the uptake of extracellularly applied WGA-HRP into intracellular organelles (Figure 2). Serial cross sections of axotomyzed neurons revealed uptake of WGA-HRP by coated pits and vesicles (Figures 2E–2G) that accumulated at the central region of the GC (Figures 2A and 2C). Profiles indicative of membrane retrieval were observed at high frequency in the neurolemma corresponding to the central region of the GC and at a lower frequency in more proximal regions. Retrieved membrane intermingled with dense vesicles accumulated at the central region of the GC (Figures 2A, 2C, and 2F) but not in regions proximal to it (Figure 2B) nor in the control intact axons. In the central region of the GC, WGA-HRP was visible in association with coated pits, coated vesicles, endosomes of various forms, and multivesicular bodies (Figures 2C–2G). Thus, the electron microscopic observation suggested that axotomy leads to increased endocytotic activity and that this activity takes place with somewhat higher frequency at the GC center. The retrieved membrane accumulates together with transported dense vesicles at the GC center.

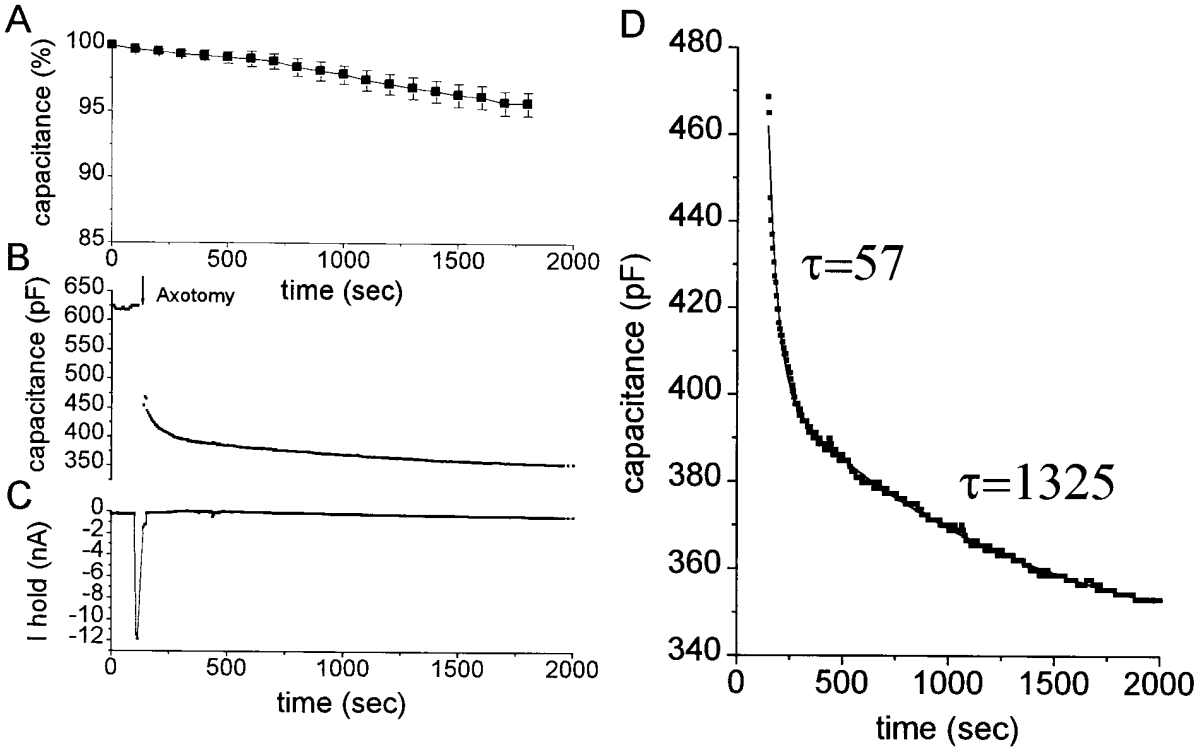

Figure 1. Membrane Capacitance Measurements in a Neuron That Did Not Extend a GC Lamellipodium Revealed That Axotomy Accelerates Membrane Retrieval

(A) The capacitance values of intact isopotential cultured neurons were normalized in respect to the first value obtained after breaking the seal. The bars represent SEM (n = 11). Note that the average decrease in membrane capacitance over a period of 30 min was less than 5%.

(B) Axonal transection of a nonisopotential cultured neuron (arrow) resulted in a sharp decrease in membrane capacitance from 640 pF to 468 pF. This decrease corresponds to the reduction of the surface area of the neuron by the elimination of the distal axonal segment.

(C) Axotomy was associated with a transient increase in the holding current that recovered to the control level as soon as a membrane seal was formed over the cut end of the axon.

(D) After the formation of a membrane seal, a decrease in membrane capacitance from 468 pF to 350 pF over a period of 30 min was recorded. The decreased capacitance can be described by two time constants of 57 and 1325 s.

Membrane Capacitance Measurements during GC Extension

In the present series of experiments, only a fraction of the patched neurons extended GCs postaxotomy (n = 18 out of a total of 47). In these cases, the tip of the transected axon extended a lamellipodium 5–10 min postaxotomy (Figures 3 and 4). In six of these experiments, the rapid extension of the lamellipodium was clearly related to an increase in the neuronal capacitance. In the rest (n = 12), while a GC was extending and the apparent visible surface area of the lamellipodium was increasing, the neuronal membrane capacitance was unexpectedly decreasing. In the following paragraphs, we will first describe the results with positive correlation between membrane capacitance and visible increase in the lamellipodial surface area and then the results in which a negative correlation was recorded.

For the experiment illustrated in Figure 3, the axon was first transected and 5 min later the neuron was patched on its cell body. Immediately after breaking the seal, the membrane capacitance transiently decreased for 100 s, (Figure 3A). Thereafter, an increase in membrane capacitance was measured while a lamellipodium was continuously extending at a rate of 120 μm^2/min (Figure 3D). An increase in membrane capacitance and in the GC's dimensions was recorded for up to 60 min postaxotomy.

To examine the relations between the visible increase in the lamellipodial surface area and the changes in membrane capacitance, we used the following procedure: First, the increase in the lamellipodial surface area was measured from video recordings and expressed in pF (assuming specific membrane capacitance of 1 $\mu F/cm^2$; Figure 3B). The correlation between the measured membrane capacitance and the surface area gave a correlation coefficient of 0.97 (Figure 3C). The slope of the correlation curve is 0.6; thus, it is reasonable to assume that in this experiment membrane retrieval was induced in parallel to exocytosis. The process of membrane retrieval in this case masked ~40% of the exocytotic activity.

It is of interest to note that extension of the GC lamellipodium, to reach a surface area of 5000 μm^2 within 20–40 min postaxotomy, corresponds to an average increase in GC surface area of 120–240 μm^2/min. Electron microscopic observations made in our laboratory (Figure 2) revealed that 90 nm diameter vesicles accumulate at the center of the GC. Assuming that these vesicles serve as the source for the GC membrane and that each

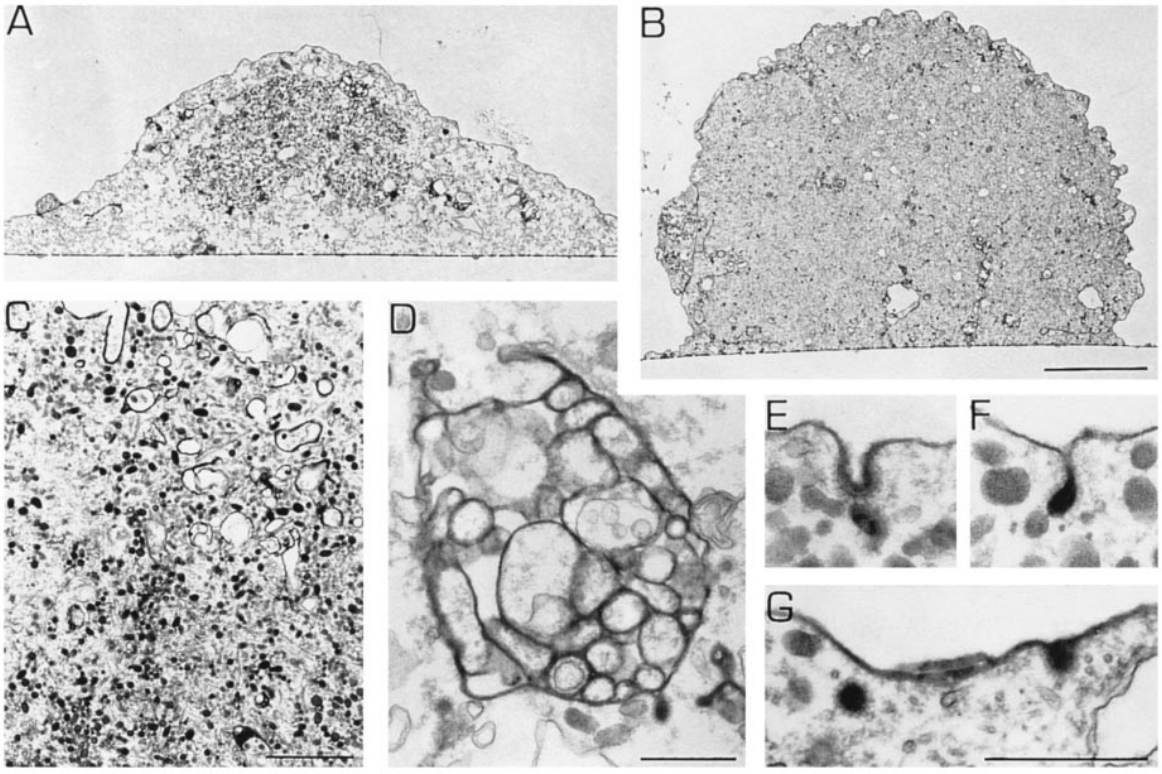

Figure 2. Cross Sections of Axotomyzed Neurons Revealed Uptake of WGA-HRP

Horseradish peroxidase conjugated to wheat germ agglutinin (WGA-HRP) was taken up into various forms of vesicles that accumulated at the central region of the GC (A). Accumulation of retrieved membrane was not observed in regions proximal to the growth cone (B). In the central region of the GC, WGA-HRP-containing organelles intermingled with dense vesicles (F) were visible in association with coated pits (E–G), coated vesicles (G), endosomes of various forms (C), and multivesicular bodies (D). Bars: in (A) and (B), 5 μm; in (C) 1.5 μm; in (D)–(G), 0.5 μm.

vesicle has a membrane surface area of 0.025 μm^2, a total of 200,000 vesicles should have fused with the neurolemma. Accordingly, the observed rate of growth corresponds to exocytosis of 80–180 vesicles per second. This rate of exocytosis is within the range of exocytotic activity that was detected in cells specialized to vigorously release hormones in response to specific stimuli (Thomas et al., 1990; Neher and Zucker, 1993; Heinemann et al., 1994; for a recent review, see Burgoyne and Morgan, 1995).

In the second group of axotomized neurons that extended lamellipodia (n = 12), capacitance measurements revealed that, while the GC lamellipodium was extending, the membrane capacitance decreased. An example of such an experiment is illustrated in Figure 4. In this experiment, cutting off the axon resulted in a decrease in membrane capacitance from an estimated value of 1250 pF to 396 pF (Figure 4A, inset). In parallel to the extension of the lamellipodium (Figure 4B), the membrane capacitance gradually decreased from 400 pF to 330 pF over a period of about 40 min (Figure 4A). The kinetics of decrease in membrane capacitance followed two time constants: an early fast time constant of 182 s and a late phase with a time constant of 2434 s.

The gradual decrease in membrane capacitance while the GC is vigorously extending a lamellipodium can be attributed to one of the following mechanisms. First, axotomy induces parallel endo- and exocytotic activity. In these neurons, an excess amount of membrane is retrieved at one location, and only a fraction of it is routed to the lamellipodium. Under these conditions, it is plausible that while the lamellipodium extends, the total surface area of the neuron decreases. A second, alternative explanation to account for the observation is that while the very flat (0.1–1 μm) lamellipodium is extending, the neuron gradually become less and less isopotential. Thus, the lamellipodium is not voltage clamped properly, and the capacitance measurements become progressively inaccurate. To examine this second hypothesis, we tested whether the capacitance measurements accurately record the increase in the lamellipodial surface area. This was done by trimming away parts of the lamellipodium while measuring the neuron's membrane capacitance and then by correlating the decrease in surface area and decrease in capacitance.

The procedure is illustrated by Figure 5 (from the same experiment as shown in Figure 4). Elimination of the upper part of the lamellipodium (Figure $5A_I$) led to a decrease in membrane capacitance from 330 pF to 319 pF, i.e., by 11 pF (Figure 5B, first arrow, open circles). The elimination of the lower part of the lamellipodium (Figure 5 A_{II}) was associated with a further decrease in membrane capacitance from 318 pF to 302 pF, i.e., by

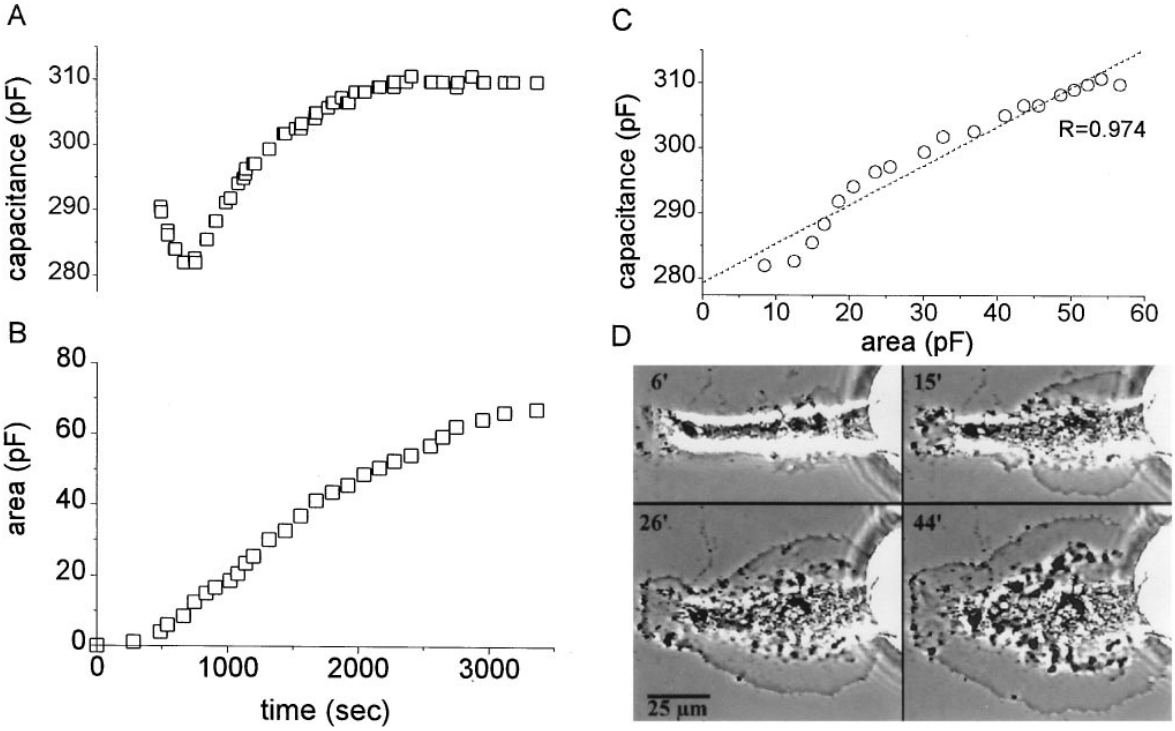

Figure 3. Correlation between the Visible Surface Area of an Extending Lamellipodium and the Measured Capacitance

For this experiment a neuron was first axotomized and only 500 s later patch clamped. The measured capacitance initially decreased for a duration of 100 s. Thereafter, the membrane capacitance increased from 282 pF to 310 pF (A). Concomitantly with the increase in membrane capacitance, the GC extended a lamellipodium (D). The increase in the visible surface area expressed in pF (assuming 1 $\mu F/cm^2$), is shown in (B). The correlation between the measured membrane capacitance (Y axis) and visible surface area (X axis) gave a correlation coefficient of 0.97 with a slope of 0.6 (C). Phase contrast images of the extending lamellipodium 6, 15, 26, and 44 min postaxotomy (D). Part of the cell body is shown on the right side of the micrographs.

16 pF (Figure 5B, second arrow, open circles). The measured decrease in membrane capacitance corresponds well to the expected reduction in the dimensions of the lamellipodium. Trimming off the upper part of the lamellipodium eliminated a surface area that should correspond to about 15 pF (Figure 5A$_I$, and open squares

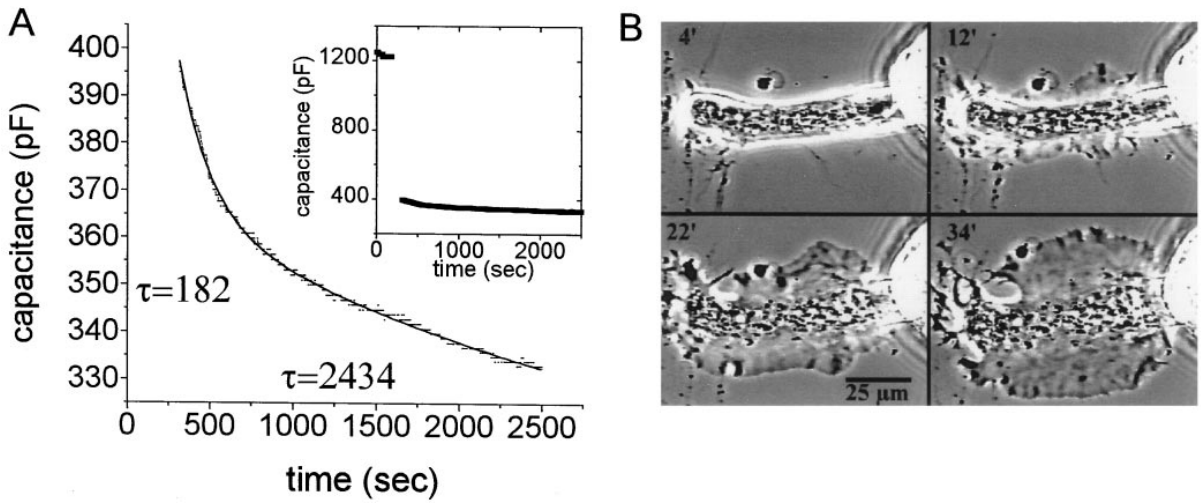

Figure 4. Decrease in Membrane Capacitance as a Function of Time Postaxotomy in a Neuron That Developed a Lamellipodium

Axonal transection resulted in a decrease in membrane capacitance from ~1250 pF to 396 pF (inset). While the GC was extending a lamellipodium (B), the membrane capacitance gradually decreased from 395 pF to 333 pF over a period of about 40 min (A). (B) Phase contrast images of the extending lamellipodium 4, 12, 22, and 34 min after axonal transection. Part of the cell body is seen on the right side of each image.

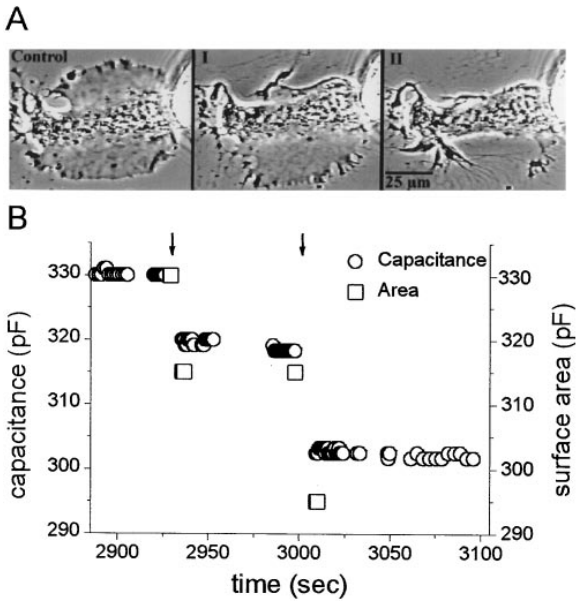

Figure 5. Correlation between Lamellipodial Surface Area and Membrane Capacitance

The membrane capacitance of an axotomized neuron that extended a GC lamellipodium was measured while parts of the lamellipodium were trimmed off. The decrease in the visualized surface area (A) and measured capacitance (B) were correlated. Images of the lamellipodium are shown in control (A, Control), and after trimming away the upper part of the lamellipodium (A_I), and the lower part (A_{II}). A step decrease in membrane capacitance was monitored concomitantly with the elimination of the upper part of the lamellipodium (B, first arrow) and the lower part (B, second arrow). Membrane capacitance measurement during the elimination of the upper part of the lamellipodium was associated with a decrease in membrane capacitance of 11 pF (B, circles). The measured decrease in the membrane capacitance was in good correlation with the expected decrease in the lamellipodial surface area expressed in pF, i.e., by 15 pF (square indicated by the first arrow in B). The second transection of the lower part of the lamellipodium was associated with a 16 pF decrease in membrane capacitance (B, second arrow). The decrease in visualized surface area corresponded to a 20 pF decrease in membrane capacitance (square indicated by the second arrow in B).

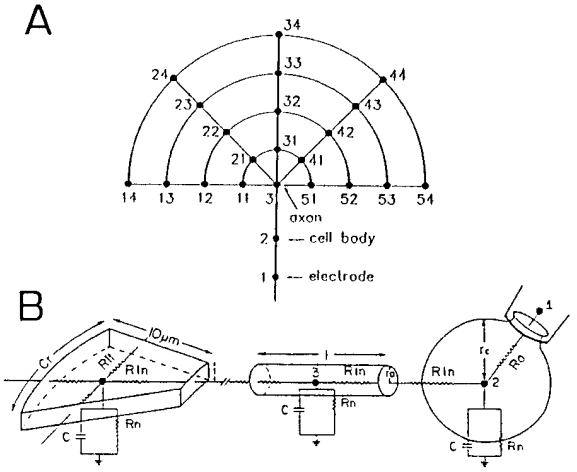

C

	Compartments	Dimentions μm	Membrane capacitance pF	Input resistance GΩ	Lontitudal resistance MΩ	Lateral resistance MΩ
	Cell body	r_c=50	314	0.16		
	Axon	l=60 r_a=7	26	1.9	0.39	
Lamellipodium compartments	11,21,31,41,51 0-10 μm	t=4	0.78	64	0.64	0.1
	12,22,32,42,52 10-20 μm	t=0.75	2.3	22	1.14	1.6
	13,23,33,43,53 20-30 μm	t=0.2	3.9	12.7	2.5	9.8
	14,24,34,44,54 30-40 μm	t=0.1	5.5	9	3.7	27

Figure 6. The Structure and Calculated Values of the Membrane and Cytoplasmic Properties Used in the Computer Simulation Model

(A) Each compartment is represented by a closed circle: the electrode resistance is represented by compartment 1 (Ra); the cell body, by compartment 2; the axon, by compartment 3; and the lamellipodium, by compartments 11–54. The connecting lines between compartments represent longitudal (Rln) or lateral resistance (Rlt) as indicated in Figure 6B. The values assigned to each compartment are detailed in (C).

The thickness of the lamellipodium is represented by t; circumference at the middle of each compartment, by Cr; axon length, by l; axon radius, by r_a; and cell body radius, by r_b. Input resistance (Rn), membrane capacitance (C), longitudal resistance (Rln), lateral resistance (Rlt).

in Figure 5B), while the second transection eliminated a surface area that should equal to 20 pF (Figure 5A_{II}, and open squares in 5B).

This experiment and others of the same kind (n = 12) demonstrated that capacitance measurements correspond to 50%–90% of the expected lamellipodium surface area when expressed in picofarads. The differences between the measured values and the calculated values from the lamellipodial surface area could be due to inaccuracies in the measurements of the surface area from the video recordings, or in the assigned value for the specific membrane capacitance.

To get a deeper insight into this problem, we used the EV-Pspice program to construct an electrical circuit simulation model of the growing transected neuron (Figure 6; see Experimental Procedures for more details). The model simulated a cell body connected through an axon to a large lamellipodium. Using this simulation model, we examined whether the neuron, along with its GC, is isopotential. This was done by analyzing the capacitance currents and the voltage drop along the modeled lamellipodial compartments. The neuron consisted of a 50 μm radius cell body, an axon with a diameter of 14 μm and length of 60 μm, and a lamellipodium with a radius of 40 μm, using the following parameters: specific membrane resistance of 50 KΩ/cm^2 (Spira, et al., 1993), specific axial resistance of 250 Ω/cm (Shelton, 1985), and specific membrane capacitance of 1 μF/cm^2 (Shelton, 1985).

The simulations revealed that there is no significant voltage drop over the lamellipodial membrane and that the capacity current can be fitted by one exponential. Thus, based on the experimental results and the computer simulation model, we conclude that the decrease in membrane capacitance recorded in parallel to the lamellipodial extension accurately reflects the values of membrane retrieval rather than being a measurement artifact.

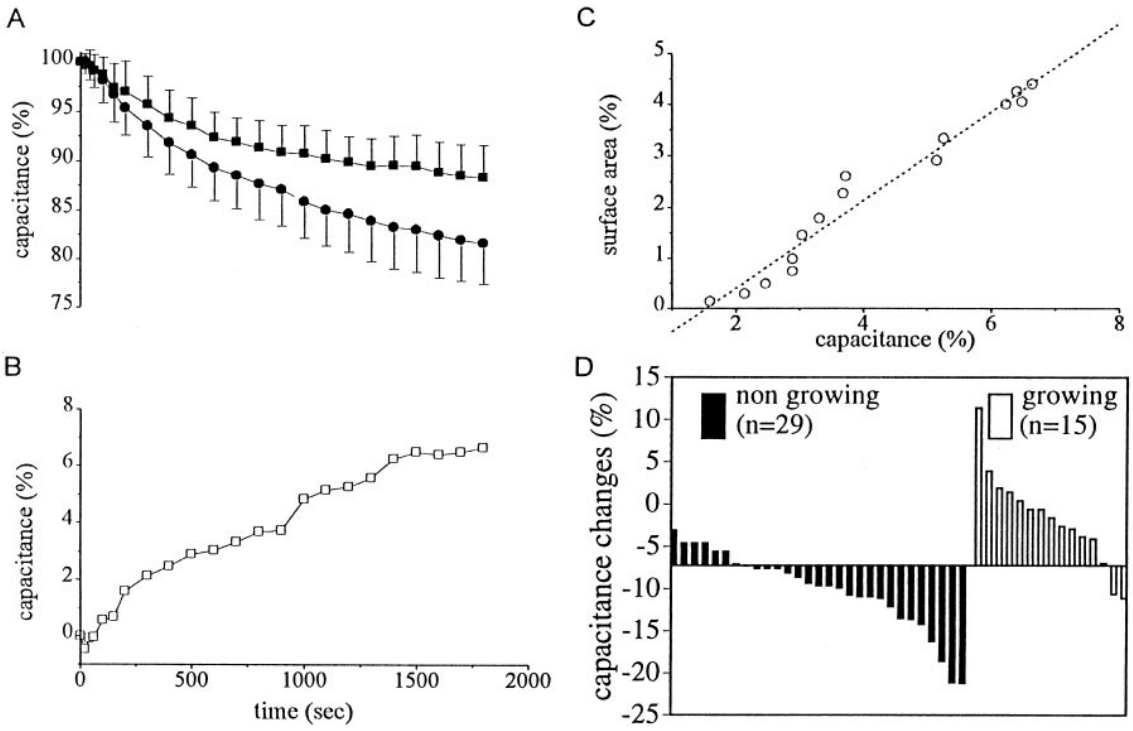

Figure 7. The Rate of Membrane Insertion during GC Extension and the Difference among the Nongrowing and the Growing Axotomized Neurons

The rate of membrane insertion (exocytosis) into the neurolemma during GC extension was estimated by subtracting the averaged decrease in membrane capacitance measured in axotomized neurons that extended lamellipodia from that in neurons that did not extend lamellipodia.

(A) Average decrease in membrane capacitance of growing neurons (squares) and nongrowing neurons (circles). The graph demonstrates that the average membrane capacitance decrease is significantly faster in the nongrowing neurons. Bars represent SD.

(B) Subtraction of the curves shown in (A) reveals the fraction of increased membrane capacitance in the growing axotomized neurons. Approximately 7% of the total area was inserted into the plasma membrane over 30 min.

(C) The correlation coefficient between the average increase in lamellipodial capacitance and the average increase in the visualized surface area of the neurons is 0.98 with a slope of 0.86.

(D) The ordinate of the horizontal line of the graph is set to the average decrease in membrane capacitance of 44 axotomized neurons 30 min postaxotomy at −7.2% (irrespective of GC extension). The net percentage changes in membrane capacitance of each of the 44 neurons was calculated and plotted. Closed columns represent the decrease in membrane capacitance of nongrowing neurons, and open columns represent the growing neurons. Note that the membrane capacitance of most of the nongrowing neurons decreased in excess of the averaged 7.2%, while the membrane capacitance of the growing neurons decreased less than the average.

Membrane Recycling Dynamics in Growing and Nongrowing Axotomized Neurons

In the majority of the experiments, axotomy was followed by decrease in membrane capacitance. The decreased capacitance was recorded in axotomized neurons that did not extend lamellipodia (n = 29), as well as in axotomized neurons that did extend lamellipodia (n = 12). Examination of the curves describing the normalized averaged values of neuron capacitance postaxotomy over time revealed that the rate and extent of decrease in membrane capacitance is significantly larger in nongrowing transected neurons than in growing neurons. This is illustrate in Figures 7A–7C, which depict only experiments in which the neurons were patched prior to axonal transection and the lamellipodial surface area could be measured from video images throughout the experiments (n = 17). This allowed us to normalize the capacitance values obtained postaxotomy with respect to the first capacitance value that was measured after the completion of membrane sealing over the cut end of the axon. Figure 7A illustrates the average decrease in membrane capacitance of growing neurons (closed squares, n = 3) and the average decrease in capacitance of nongrowing neurons (closed circles, n = 14). The kinetics of the decrease in membrane capacitance of the two groups of neurons is significantly different (by two-way analysis of variance, $p < .001$), and the nongrowing neurons reveal a faster rate of membrane retrieval.

Assuming that in the nongrowing neurons the exocytotic activity occurs at a much slower rate than membrane retrieval, and that in growing neurons exocytosis is more vigorous yet not a dominant process, then the subtraction of the two curves should provide an estimated rate of new membrane incorporation into the extending lamellipodium. As shown in Figure 7B, ~6.6% new membrane is incorporated into the neurolemma over a period of 30 min at an averaged rate of 0.25%/min in the neurons that extended lamellipodia. For the neurons in Figure 7A, the increase in lamellipodial sur-

face area was measured from video recording, and the average increase in lamellipodial surface area was calculated. The correlation coefficient between the average increase in the visualized lamellipodial surface area and the calculated increase in membrane capacitance shown in Figure 7B is 0.98 with a slope of 0.86 (Figure 7C).

To emphasize the difference in membrane capacitance measurements among the nongrowing and growing axotomized neurons, we used the following presentation. The average changes in membrane capacitance postaxotomy of all the neurons ($n = 44$) was calculated and found to be 11.6%. As mentioned earlier (Figure 1A), 4.4% of the decreased capacitance is attributed to the subtle increase in endocytosis following the rupturing of the cell membrane by the patch electrode; thus, axotomy induced on the average a 7.2% decrease in membrane capacitance over a period of 30 min (ordinate of the horizontal line of Figure 7D). Most of the nongrowing neurons lost more than 7.2% of their membrane capacitance (average decrease of 10.3%; SD = 4.6; $n = 29$; Figure 7D, closed columns). The growing neurons, except for two, lost less than 7.2%, i.e., an average of 1.7% (SD = 4.9; $n = 15$; Figure 7D, open columns). This presentation of the data clearly illustrates the differences between the populations of nongrowing and growing axotomized neurons and supports the interpretation that, although membrane retrieval is the dominant process in both groups, in the growing neurons exocytotic activity contributes to the overall changes in the surface membrane area.

Earlier studies of transected axons revealed structural indications for enhanced endocytotic activity at the region of the sealed end of the transected axon (Fishman et al., 1990). Likewise, structural and biochemical experiments suggested that endo- and exocytotic activities simultaneously take place in GCs (Bray, 1973; Wessells et al., 1974; Bunge, 1977; Cheng and Reese, 1987). The membrane capacitance measurements of the present study are consistent with these observations in demonstrating that both membrane retrieval and exocytosis occur simultaneously in the regenerating cut end during the initial period following axotomy and GC extension. Furthermore, our study revealed the surprising fact that, shortly after axotomy and during the initial phases of lamellipodial extension, membrane retrieval rather than the addition of new membrane to the neurolemma is the dominant process. Thus, while the visible surface area of the GC increases, the total surface area of the transected neuron decreases. The simultaneous recordings of decreased membrane surface area and vigorous extension of the GC lamellipodium imply that the sites of membrane retrieval and exocytosis must be spatially remote. Electron microscopic observation suggests that endocytotic activity occurs mainly (but not exclusively) at the GC center and that the retrieved vesicles accumulate together with transported dense vesicles at the GC center. The precise site of intracellular membrane fusion with the axolemma was not determined yet.

The excess membrane retrieval over exocytosis following axotomy may play an important role in the early response of neurons to axotomy. Thus, the rapidly retrieved membrane might establish an immediate reservoir for rapid growth after injury. Retrieved membrane in the form of vesicles can also carry "injury"-related signals from the injured site to the nucleus (Gunstream et al., 1995). It is of interest to note that accelerated endocytotic activity was documented by electron microscopic observations following the exposure of cultured Aplysia sensory neurons to serotonin (Bailey et al., 1992). Bailey and Kandel and their coworkers (Bailey et al., 1992; Hu et al., 1993) suggested that serotonin-induced endocytosis down-regulates the density of membrane adhesion molecules and thereby promotes the detachment of neurites from the substrate. This detachment is an essential step in a cascade of events that leads to re-growth of adult neurons in relation to long-term neuronal plasticity induced by serotonin (Bailey and Kandel, 1993).

The mechanisms that trigger membrane retrieval and addition of membrane postaxotomy are not known. Recent studies suggest that an increase in the intracellular calcium concentration to 50–200 μM in chromaffin cells and melanotrophs accelerates membrane retrieval, whereas at low micromolar calcium concentrations exocytotic activity is induced (Thomas et al., 1990; Neher and Zucker, 1993; Heinemann et al., 1994; Thomas et al., 1994; Burgoyne and Morgan, 1995). Axotomy of cultured Aplysia neurons elevates the free intracellular calcium concentration from $\sim$100 nM to the millimolar range for a duration of a few minutes (Ziv and Spira, 1995). Since membrane retrieval was monitored postaxotomy for over 30 min, it is unlikely that the elevated calcium concentration is necessary for the perpetuation of the process. It is, however, possible that the transient elevation in the free intracellular calcium concentration triggers the process.

The present study demonstrates that axotomy rapidly alters the balance between endo- and exocytotic activities of cultured adult neurons. The immediate response of the neuron to axotomy is the parallel activation of membrane retrieval and exocytosis. The rapid and dominant activation of membrane retrieval mechanisms establishes an available membrane store that might support the rapid initial stages of GC formation and extension.

Experimental Procedures

Cell Culture

Either juvenile specimens of Aplysia californica or adult Aplysia oculifera collected from the northern section of the Gulf of Eilat, Israel, were used. Culturing procedures were carried out as previously described (Schacher and Proshansky, 1983; Benbassat and Spira, 1993; Spira et al., 1993; Ziv and Spira, 1993, 1995). In brief, abdominal ganglia were isolated and incubated for 1.5–2.5 hr in 1% protease (Sigma type IX) at 35°C. The ganglia were then desheathed, and the cell body of the Rb neurons (Kandel, 1976) with their long axons were pulled out with sharp micropipettes and placed on poly-L-lysine- (Sigma) coated glass-bottomed culture dishes. For some of the experiments, we grew the neurons on a noncoated glass bottom. Under these conditions, the isolated neurons did not extend neurites; the main axon shrank; and thus many of the neurons became a compact isopotential structure. The culture medium consisted of equal parts of filtered hemolymph from Aplysia faciata collected along the Mediterranean coast and L-15 supplemented for marine species (Spira et al., 1993; Ziv and Spira, 1993, 1995).

Axotomy

Axonal transection was performed, as previously described, by applying pressure on the axon with the sharpest shaft of a micropipette under visual control (Benbassat and Spira, 1993, 1994; Spira

et al., 1993; Ziv and Spira, 1993, 1995). The experiments were performed after replacement of the culturing medium by artificial sea water composed of 460 mM NaCl; 10 mM KCl; 10 mM $CaCl_2$; 55 mM $MgCl_2$; 10 mM HEPES (adjusted to pH 7.6).

Membrane Capacitance Measurement

Capacitance measurement were made with the EPC-9 (Heka Electronics, Lambrecht, Germany) using the time-domain technique in the whole-cell configuration (Hamill et al., 1981, Lindau and Neher, 1988). Boralex pipettes (Rochester Scientific) were pulled with a PP-83 Narashige puller and fire polished to get a 1 MΩ resistance. Pipette solutions contained 400 mM Cesium Glutamate, 20 mM NaCl, 2 mM $MgCl_2$, 80 mM CsCl, 60 mM HEPES, 0.250 mM EGTA, 10 mM ATP, 0.5 mM GTP (adjusted to pH 7.15). Under these conditions the free intracellular calcium concentration was between 50 and 100 nM. Neurons were patched on the cell body. After obtaining a gigaohm seal, the pipette capacitance was compensated. The membrane under the patch was ruptured to get a low access resistance (2–5 MΩ) to the inside of the cell.

The neurons were voltage clamped to values near their resting potential (−50 mV), and the membrane capacitance was automatically compensated every few seconds by the EPC-9 Cslow compensation mode. Pulse data were stored on an Atari STE-4 computer, filtered at 2.3 KHz, and analyzed with the Review program (Heka Electronics, Lambrecht, Germany).

Prior to axonal transection, most neurons were not isopotential. Thus, the membrane capacitance values prior to axotomy are an underestimate of the real value. Only after axotomy, when a large portion of the neuron was trimmed away, did the neurons become an isopotential structure. Isopotentiality of the neuron was verified as follows: a square hyperpolarization pulse with a duration of 30 ms and an amplitude of -10 mV was applied to the cell while the auto-Cslow was not operating. The corresponding current was then analyzed by fitting the transient current (which is basically a capacity current) by one exponential. This procedure was repeated throughout the experiment to assure that the neuronal structure remained isopotential even when a GC lamellipodium was extending. The holding current, the input resistance of the neuron, and the access resistance of the patch electrode were continuously monitored throughout the experiments. Changes in these parameters were not in correlation with changes in membrane capacitance and are not shown. Whenever the changes exceeded the following parameters, the experiment was discontinued and excluded from analysis: input resistance <100 MΩ, access resistance >5 MΩ, and holding current >−400 pA. The experiments were carried out at room temperature ranging between 20°C and 24°C. Experiments were performed on neurons 7–24 hr after culturing.

Electron Microscopy

The sites of membrane retrieval and the accumulation of retrieved membrane postaxotomy were identified by the uptake of extracellularly applied WGA-HRP into intracellular organelles (Watson and Burrows, 1981). For the experiment, the cultured neurons were incubated in 2% WGA-HRP artificial sea water solution for 30 min. Then, after a thorough wash of the excess WGA-HRP by 50–80 ml artificial sea water, the axon was transected and maintained in artificial sea water for a period of 30–40 min. During this period, the cut end recovered and extended a lamellipodium. The transected neuron was then fixed and processed to allow the production of an electron-dense deposit by the HRP as previously described (Watson and Burrows, 1981). Control experiments in which cultured neurons were exposed to the above-mentioned procedures revealed that intact neurons do not show endogenous HRP activity and that the rate of WGA-HRP uptake by intact axons is negligible in respect to that seen after axotomy.

Simulation Model for GC Extension

A computer simulation program to model the passive electrical properties of a transected neuron was designed using the EV-Pspice program (MicroSim Corp.). The model was designed to represent the cell body and an axon that extends from its tip a large lamellipodium. The simulation model was constructed from 54 compartments (Figure 6A, closed circles). The input resistance and capacitance of each compartment was represented by a resistor (Rn) and capacitor (C) in parallel. Each compartment was connected to its neighboring compartments by a resistor representing the cytoplasmic resistance (Rln and Rlt; see Figures 6A and 6B, lines). The structure of the model is given in Figures 6A and 6B, and the values of each compartment are detailed in Figure 6C. The electrode's access resistance of 5 MΩ is represented by compartment 1 (as Ra); the cell body, by compartment 2; the axon, by compartment 3; and the lamellipodium, by compartments 11–54. The values of resistance (Rn) and capacitance (C) assigned to each compartment were calculated to correspond to the morphological dimensions of each compartment (Figure 6C) using specific membrane resistance of 50 KΩ/cm^2 (Shelton, 1985; Spira et al., 1993), specific axial resistance of 250 Ω/cm (Shelton, 1985), and specific membrane capacitance of 1 μF/cm^2 (Shelton, 1985). The cytoplasmic resistance between compartments was calculated to correspond to the thickness of the lamellipodium as revealed by electron micrographs obtained in our laboratory (data not shown).

The values for a cell body of 50 μm radius, an axon with a diameter of 14 μm and length of 60 μm, and a lamellipodium with a radius of 40 μm are given in Figure 6C and were calculated according to the following formulas:

Cell body: surface area: $S = 4\pi r_c^2$, r_c represents cell radius; membrane capacitance: $C = C_m \cdot S$; input resistance: $R_n = Rm/S$.

Axon: surface area: $S = 2\pi r_a l$, l represents the axon length and r_a represents the axon radius; membrane capacitance: $C = C_m \cdot S$; input resistance: $R_n = Rm/S$; longitudal resistance: $Rln = (Ri \cdot l)/a$, a represents the axon cross section ($a = \pi r_a^2$).

Lamellipodium compartments: surface area: $S = (\pi x^2) \cdot 2/8$, x represents the compartment radius changing from 10–50 μm; membrane capacitance: $C = C_m \cdot S$; input resistance: $Rn = Rm/S$; longitude resistance (between points 11–12, 12–13, etc.): $Rln = (Ri \cdot 10\ \mu m)/a$ (10 μm length of each compartment), a is the cross section in the middle of each compartment, which is determined according to the circumference (Cr) in the middle of each compartment ($a = Cr \cdot t$), and t is the thickness of each compartment (as detailed in Figure 6C).

The lateral resistance (between point 11–21, 12–22, etc.): $Rlt = (Ri \cdot Cr)/a'$, a′ represents the lateral cross section ($a' = t \cdot 10\ \mu m$).

For the simulation we applied a 10 mV square voltage pulse to the cell body and analyzed the capacitance currents and the voltage drop along the compartments representing the lamellipodium. We analyzed to what extent the model deviates from isopotentiality by examining whether a transient capacitance current follows a single exponent and to what extent the voltage applied to the cell body decays over the modeled lamellipodium.

For a 10 mV voltage pulse delivered to the cell body, the voltage was attenuated between the axon (compartment 3) and the most distal compartment of the lamellipodium (point 34) by 0.01 mV. The capacity current could be fitted by one exponential (data not shown). The calculated capacitance from the current integral corresponds to 91% of the actual neuron's capacitance. Using the above-mentioned experimental parameters, the neuron is isopotential for as long as the lamellipodial diameter is <80 μm.

When the same procedure was applied assuming that Ri = 1000 Ω/cm, the simulation model indicates that the neuron maintains isopotentiality when the lamellipodium reaches a diameter of 40 μm.

Video Microscopy

To correlate between the dimensions of the lamellipodium and the membrane capacitance, video images were continuously recorded. The images were collected with a Vidicon video camera (Hamamatsu) and stored during the experiment to a video cassette recorder (Sony). Still images were formed after the experiments by averaging 7 video frames with a frame grabber (Imaging Technologies), followed by the subtraction of an out-of-focus image of an empty area of the culture dish, and the contrast was adjusted using software written in our lab. The final images were prepared using commercially available software (Adobe Photoshop). GC surface area was measured every 2 min from the video images.

Acknowledgments

We thank Prof. Erwin Neher for reviewing an earlier version of the manuscript and Ms. A. Dormann for her excellent assistance. This study was initially supported by a grant from the German Israel Foundation for Scientific Research and Development (#I56–235), and at later stages by a grant from the USA–Israeli Binational Science Research Foundation (#93–132). M. E. Spira is the Levi DeViali Professor in neurobiology.

The costs of publication of this article were defrayed in part by the payment of page charges. This article must therefore be hereby marked *"advertisement"* in accordance with 18 USC Section 1734 solely to indicate this fact.

Received August 16, 1995; revised January 5, 1996.

References

Baas, P.W., and Heidemann, S.R. (1986). Microtubule reassembly from nucleating fragments during the regrowth of amputated neurites. J. Cell Biol. *103*, 917–927.

Bailey, C.H., and Kandel, E.R. (1993). Structural changes accompanying memory storage. Annu. Rev. Physiol. *55*, 397–426.

Bailey, C.H., and Kandel, E.R. (1994). Structural changes underlying long-term memory storage in *Aplysia*: a molecular perspective. Semin. Neurosci. *6*, 35–44.

Bailey, C.H., Chen, M., Keller, F., and Kandel, E.R. (1992). Serotonin-mediated endocytosis of apCAM: an early step of learning-related synaptic growth in *Aplysia*. Science *256*, 645–649.

Bandtlow, C.E., Schmidt, M.F., Hassinger, T.D., Schwab, M.E., and Kater, S.B. (1993). Role of intracellular calcium in NI-35-evoked collapse of neuronal growth cones. Science *259*, 80–83.

Benbassat, D., and Spira, M.E. (1993). Survival of isolated axonal segments in culture: morphological, ultrastructural, and physiological analysis. Exp. Neurol. *122*, 295–310.

Benbassat, D., and Spira, M.E. (1994). The survival of transected axonal segments of cultured *Aplysia* neurons is prolonged by contact with intact nerve cells. Eur. J. Neurosci. *6*, 1605–1614.

Bray, D. (1970). Surface movements during the growth of single explanted neurons. Proc. Natl. Acad. Sci. USA *65*, 905–910.

Bray, D. (1973). Model for membrane movements in neuronal growth cone. Nature *244*, 93–96.

Bray, D. (1992). Cytoskeletal basis of nerve axon growth. In The Nerve Growth Cone, P.C. Letourneau et al., eds. (New York: Raven Press), pp. 7–17.

Bray, D., Thomas, C., and Shaw, G. (1978) Growth cone formation in cultures of sensory neurons. Proc. Natl. Acad. Sci. USA *75*, 5226–5229.

Bunge, M.B. (1977). Initial endocytosis of peroxidase or ferritin by growth cones of cultured nerve cells. J. Neurocytol. *6*, 407–439.

Burgoyne, R.D., and Morgan, A. (1995). Ca^{2+} and secretory dynamics. Trends Neurosci. *18*, 191–196.

Ceccarelli, B., Hurlbut, W.P., and Mauro, A. (1973). Turnover of transmitter and synaptic vesicles at the frog neuromuscular junction. J. Cell Biol. *57*, 499–524.

Cheng, T.P.O., and Reese, T.S. (1987). Recycling of plasmalemma in chick tectal GCs. J. Neurosci. *7*, 1752–1759.

Fawcett, W.F., and Keynes, R.J. (1990). Peripheral nerve regeneration. Annu. Rev. Neurosci. *13*, 43–60.

Feldman, E.L., Axelrod, D., Schwartz, M., Heacock, A.M., and Agranoff, B.W. (1981). Studies on the localization of newly added membrane in growing neurites. J. Neurobiol. *12*, 591–598.

Fernandez, J.M., Neher, E., and Gomperts, B.D. (1984). Capacitance measurements reveal stepwise fusion events in degranulating mast cells. Nature *312*, 453–455.

Fishman, H.M., Tewari, K.P., and Stein, P.G. (1990). Injury-induced vesiculation and membrane redistribution in squid giant axon. Biochem. Biophys. Acta *1023* 421–435.

Griffin, J.W., Price, D.L., Drachman, D.B., and Morris, J. (1981). Incorporation of axonally transported glycoproteins into axolemma during nerve regeneration. J. Cell Biol. *88*, 205–214.

Gunstream, J.D., Castro, G.A., and Walters, E.T. (1995). Retrograde transport of plasticity signals in *Aplysia* sensory neurons following axonal injury. J. Neurosci. *15*, 439–448.

Hamill, O.P., Marty, A., Neher, E., Sakman, B., and Sigworth, F.J. (1981). Improved patch-clamp techniques for high resolution current recording from cells and cell-free membrane patch. Pflügers. Arch. *391*, 85–100.

Haydon, P.G., McCobb, D.P., and Kater, S.B. (1987). The regulation of neurite outgrowth, growth cone motility, and electrical synaptogenesis by serotonin. J. Neurobiol. *18*, 197–215.

Heinemann, C., Chow, R.H., Neher, E., and Zucker, R.S. (1994). Kinetics of secretory response in bovine chromaffin cells following flash photolysis of caged Ca^{2+}. Biophys. J. *67*, 2546–2557.

Heuser, J.E., and Reese, T.S. (1973). Evidence for recycling of synaptic vesicle membrane during transmitter release at the frog neuromuscular junction. J. Cell Biol. *57*, 315–344.

Hochner, B., and Spira, M.E. (1987). Preservation of motorneuron electronic characteristics during postembryonic growth. J. Neurosci. *7*, 261–270.

Hu, Y., Barzilai, A., Chen, M., Bailey, C.H., and Kandel, E.R. (1993). 5-HT and cAMP induce the formation of coated pits and vesicles and increase the expression of clathrin light chain in sensory neurons of Aplysia. Neuron *10*, 921–929.

Johnston, R.N., and Wessells, N.K. (1980). Regulation of the elongating nerve fiber. Curr. Top. Dev. Biol. *16*, 165–206.

Kandel, E.R. (1976). Cellular Basis of Behavior (San Francisco: Freeman).

Kater, S.B., and Mills, L.R. (1991). Regulation of growth cone behavior by calcium. J. Neurosci. *11*, 891–899.

Keynes, R.J., and Cook, G.M.W. (1992). Repellent cues in axon guidance. Curr. Opin. Neurobiol. *2*, 55–59.

Krause, T.L., Fishman, H.M., Ballinger, M.L., and Bittner, G.D. (1994). Extent and mechanism of sealing in transected giant axons of squid and earthworms. J. Neurosci. *1*, 6638–6651.

Lindau, M., and Neher, E. (1988). Patch-clamp techniques for time resolved capacitance measurements in single cells. Pflügers. Arch. *411*, 137–146.

Lindau, M., Stuenkel, E.L., and Nordmann, J.J. (1992). Depolarization, intracellular calcium and exocytosis in single vertebrate nerve ending. Biophys. J. *61*, 19–30.

Lucas, J.H., Gross, G.W., Emery, D.G., and Gardner, C.R. (1985). Neuronal survival or death after dendrite transection close to the perikaryon: correlation with electrophysiologic, morphologic, and ultrastructural changes. Centr. Nerv. Sys. Trauma *2*, 231–255.

Marsh, M., and Helenius, A. (1980). Adsorptive endocytosis of semliki forest virus. J. Mol. Biol. *142*, 439–454.

Matteoli, M., Takei, K., Perin, M.S., Sudhof, T.C., and De Camilli, P. (1992). Exo-endocytotic recycling of synaptic vesicles in developing processes of cultured hippocampal neurons. J. Cell Biol. *117*, 849–861.

Neher, E., and Zucker, R.S. (1993). Multiple calcium-dependent processes related to secretion in bovine chromaffin cells. Neuron *10*, 21–30.

Penner, R., and Neher, E. (1989). The patch-clamp technique in study of secretion. Trends Neurosci. *12*, 159–163.

Pfenninger, K.H., and Friedman, L.B. (1993). Sites of plasmalemmal expansion in growth cones. Brain Res. *71*, 181–192.

Popov, S., Brown, A., and Poo, M.M. (1993). Forward plasma membrane flow in growing nerve processes. Science *259*, 244–246.

Schacher, S., and Proshansky, E. (1983). Neurite regeneration by *Aplysia* neurons in dissociated cell culture: modulation by *Aplysia* hemolymph and the presence of the initial axonal segment. J. Neurosci. *3*, 2403–2413.

Shaw, G., and Bray, D. (1977). Movement and extension of isolated growth cones. Exp. Cell Res. *104*, 55–62.

Shelton, D.P. (1985). Membrane resistivity estimated for the Purkinje neuron by means of a passive computer model. Neurosci. *14*, 111–131.

Spira, M.E., Benbassat, D., and Dormann, A. (1993). Resealing of the proximal and distal cut ends of transected axons: electrophysiological and ultrastructural analysis. J. Neurobiol. *24*, 300–316.

Thomas, P., Surprenant, A., and Almers, W. (1990). Cytosolic Ca^{2+}, exocytosis, and endocytosis in single melanotrophs of the rat pituitary. Neuron *5*, 723–733.

Thomas, P., Lee, A.K., Wong, J.G., and Almers, W. (1994). A triggered mechanism retrieves membrane in seconds after Ca^{2+}-stimulated exocytosis in single pituitary cells. J. Cell Biol. *124*, 667–675.

Watson, A.D.H., and Burrows, M., (1981). Input and output synapse on identified motor neurones of a locust revealed by the intracellular injection of horseradish peroxidase. Cell Tissue Res. *215*, 325–332.

Wessells, N.K., Luduena, M.A., Letourneau, P.C., Wrenn, J.T., and Spooner, B.S. (1974). Thorotrast uptake and transit in embryonic glia, heart fibroblasts and neurons in-vitro. Tissue and Cell *6*, 757–776.

Wessells, N.K., Johnson, S.R., and Nuttall, R.P. (1978). Axon initiation and GC regeneration in cultured motor neurons. Exp. Cell Res. *117*, 335–345.

Ziv, N.E., and Spira, M.E. (1993). Spatiotemporal distribution of Ca^{2+} following axotomy and throughout the recovery process of cultured *Aplysia* neurons. Eur. J. Neurosci. *5*, 657–668.

Ziv, N.E., and Spira, M.E. (1995). Axotomy induces a transient and localized elevation of the free intracellular calcium concentration to the millimolar range. J. Neurophysiol. *74*, 2625–2637.